

Delineation of ischemic lesion from brain MRI using Symmetric Bit Plane Pattern and Curvelet Co-occurrence Matrix

Karthik. R, R. Menaka

Abstract: Developing a precise segmentation algorithm to delineate ischemic lesion from brain MRI is a challenging research issue in the field of medical image analysis and neuro-radiology. These lesions are generally complex in nature and exhibit heterogeneity in their intensity profile and morphological properties. To address these challenges, a novel segmentation algorithm using Symmetric Bit Plane Pattern analysis is presented in this work. Unlike the classical segmentation algorithms which fail to extract the region of interest in the presence of scattered structures with intensity in-homogeneities, the proposed segmentation algorithm considers the left-right symmetry property of the brain for better estimation of segmentation parameters. An adaptive filter function is designed based on the gray level profile of the brain tissues to segment the intended region of interest. Once the region of interest is delineated, multi scale co-occurrence matrix based features in Curvelet space are extracted and its significance in detection of ischemic lesion is highlighted. Finally, Support Vector Machine is used to train the learning model for classification. Experimental results of the proposed work have obtained better classification accuracy of 98.8%.

Index Terms: About four key words or phrases in alphabetical order, separated by commas.

I. INTRODUCTION

Stroke is usually caused due to the interruption of blood supply to the brain. This restriction in the flow of blood is either due to rupture of blood vessels inside the brain (haemorrhage) or due to occluded blood vessels (Ischemia) [1]. The initial treatment in acute ischemic stroke focus on restoring these occluded blood vessels by applying intravenous thrombolysis. But this process will be effective only within 4½ hours after symptom onset [2]. Also, it was reported that nearly 2 million neurons might die every minute due to ischemic stroke [3]. Hence, this diagnosis and treatment requires timely intervention from experts in neuro-radiology. Estimating the volume of infarction in a fast and on-site manner would be highly desirable especially with respect to DAWN criteria. Though brain imaging techniques like Computed Tomography (CT) or Magnetic Resonance Imaging (MRI) provide a means to identify the cause of blockage, it also acts as a vital aid to estimate the risk of

complication. When compared to CT, MRI is more sensitive to identify acute ischemic infarction. Different approaches were presented in the last two decades to detect ischemic lesion with the help of semi-automatic and automatic methods [4-8]. Nabizadeh et al. introduced a scheme to segment the hyper intense lesions due to tumor and ischemic stroke using histogram based optimization method [9]. Another approach for lesion segmentation using region growing approach combined with refinement phase was introduced in [10]. Bianca et al. developed a semi-automated approach to segment the stroke lesion by combining iterative intensity maxima-based region growing with manually selected clusters of interest [11]. Ghosh et al. analysed three different segmentation approaches for lesion segmentation and concluded that Symmetry Integrated Region Growing (SIRG) based method was better when compared to the other two methods [12]. This work gives a significant cue that, symmetrical properties between the left and right portion of the brain can be used for efficient segmentation of abnormal regions from the brain. Regardless of the number of proposed methods, an ideal method to segment the ischemic lesions from brain MRI has not yet been developed. This is due to the complex dynamic varying nature of the lesion patterns.

After identifying the necessary region of interest from an input image, the next step is to characterize its properties using significant feature primitives for effective classification. Feature primitives generally extract colour, shape or texture based information to describe the identified region of interest. With respect to medical images, texture based information can serve as an optimal feature primitive to efficiently characterize the regions. Gray Level Co-Occurrence Matrix (GLCM) based features is generally used to describe the texture properties of an image in the spatial domain. An approach for computer-aided detection of ischemic lesion using GLCM features was presented by Hema Rajini et al. [13]. Asti Subudhi et al. presented a method for delineating the stroke lesion with the help of watershed transform and GLCM features [14]. As the nature of the texture pattern in brain tissues are highly complex, it can be examined well in the transform domain. If these images are decomposed into different levels of resolution, then the feature primitives can be extracted as signals of varying strength [15]. Discrete Wavelet transform is a widely used transform domain technique for feature characterization in medical images [16-20]. It basically decomposes an image into a set of high and low pass bands. These bands extract the structural detail along three directions.

Manuscript published on 30 March 2019.

*Correspondence Author(s)

Karthik. R., School of Electronics Engineering, VIT Chennai Campus, Chennai, India.

R. Menaka. School of Electronics Engineering, VIT Chennai Campus, Chennai, India.

© The Authors. Published by Blue Eyes Intelligence Engineering and Sciences Publication (BEIESP). This is an open access article under the CC-BY-NC-ND license <http://creativecommons.org/licenses/by-nc-nd/4.0/>.

But these three linear directions are highly limiting and may not characterize the directional information from brain tissues in an optimal way. Candes et al. introduced another transform called Curvelet transform which will capture the directional information of image. It could represent the curve singularity information in an optimal way [21]. Curvelet transformation is now widely in medical image processing to study the varying structural information in anatomical structures [21-23].

After extracting the important features from the segmented region, it should be trained using suitable learning algorithm for classification. These classification models are developed with multiple algorithms like Artificial Neural Networks (ANN), Decision trees and forests, Support Vector Machines (SVM), and so on. An approach was presented for segmentation of acute infarction using probabilistic neural network and adaptive gaussian mixture model [24]. Gupta et al. introduced an approach using ANN to detect the presence of ischemic lesion using texture features [25]. But ANN might often converge on local minima. Hence sometimes, it might face over fitting problem. The Support Vector Machine (SVM) is another widely employed algorithm for classifying the image features. An approach to anticipate symptomatic intracranial haemorrhage was developed by combining imaging and clinical features with SVM [26]. Another approach is presented by combining first order Curvelet features with SVM for predicting the presence of ischemic lesion [27].

In summary, the segmentation approach applied for ischemic lesion delineation should be independent of the varying intensity profiles of the lesion. Also, these regions will not always be a single connected region and it might be scattered into distinct sub regions. Hence, the conventional region based segmentation algorithms will fail if the structure of the lesions is scattered into different regions. The proposed work is oriented towards developing an efficient scheme for delineating such abnormal structures. It also addresses the need for determining good characterization scheme such that the abnormal structures segmented can be validated well with the help of significant feature primitives.

II. MATERIALS AND METHOD

Materials

The MRI datasets used in this research were collected from Global Health City, Chennai. Out of the 10 datasets, 4 were normal datasets and the remaining 6 had radiological evidence of ischemic stroke. In addition to these datasets, benchmark datasets were also utilized in this study to examine the varying nature of the ischemic lesions [28]. All these datasets were acquired in Digital Imaging and Communication in Medicine (DICOM) format and it is of 16-bit length. The proposed research work is carried out in Intel(R) i5 processor and the execution environment is MATLAB R2012b.

Processing Pipeline

The proposed work combines Symmetric Bit Plane Pattern based Segmentation (SBPPS) with Curvelet co-occurrence matrix features for detection and delineation of ischemic lesion. Initial pre-processing is done to remove the bony structures using skull stripping. Then, median filter is applied to remove the impulse noise present in the input image. SBPPS is then applied to isolate the region of interest. To

effectively quantify and represent the extracted region, co-occurrence matrix based features are extracted in Curvelet space. The features are then fed as input to the SVM for classification. Fig. 1 presents the processing pipeline of the proposed work.

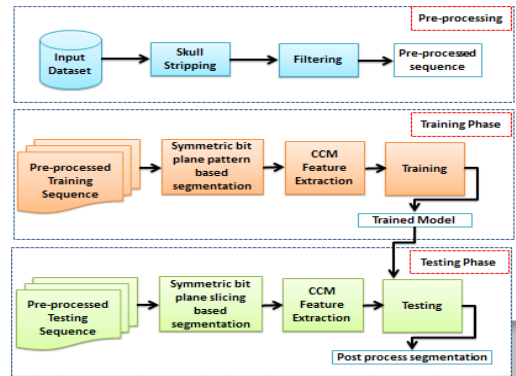


Fig. 1 Processing pipeline of the proposed work.

Symmetric Bit Plane Pattern based Segmentation

The human brain morphologically exhibits a high level of bi-fold symmetry i.e. the contents of the left and right hemisphere are almost similar in nature. This symmetrical co-existence is violated, if there is any abnormality present in the brain due to different pathological conditions [29]. Radiologists generally utilize symmetry/asymmetry as one of the differentiating features to assess abnormalities in brain images. In the recent few years, researchers are motivated to utilize this symmetry based model to detect and localize the presence of brain lesions. This research aims at developing an efficient approach for segmentation of brain lesion using left-right symmetry of the brain. The input image is bifurcated into two halves by finding the adaptive midline of the brain image i.e. based on the structure of the MRI slice, it will find the midpoint of the brain portion along each row and then, a curve is traced based on the identified midpoints to bifurcate the given slice into left and right halves. The results of the bifurcation step for a sample MRI slice are presented in Fig. 2. Then, bit plane slicing is applied to the left and right halves. The formation of bit plane ‘BP’ for the ‘kth’ bit in image $I(x, y)$ is given by Eq. 1.

$$BP_{k(x,y)} = \text{Remainder} \left(\frac{1}{2} \left[\left(\frac{1}{2^{k-1}} \right) * I(x,y) \right] \right) (1)$$

where $[x]$ represents floor function of x and ‘k’ varies from 1 to 16.

For each plane, the difference between the count of white pixels present in the left and right section is calculated as presented in Eq. 2

$$D_Count_k = \left| \left(\sum_{x=1}^m \sum_{y=1}^n BP_Left_{k(x,y)} \right) - \left(\sum_{x=1}^m \sum_{y=1}^n BP_right_{k(x,y)} \right) \right| (2)$$

where ‘m x n’ refers to the size of the image.

This will provide a good estimate on the intensity distribution of the bit plane, in which the content relatively varies between the left and the right portion of the brain slice. The planes which possess the maximum degree of dissimilarity are further utilized to isolate the required region of interest in the next step of segmentation.

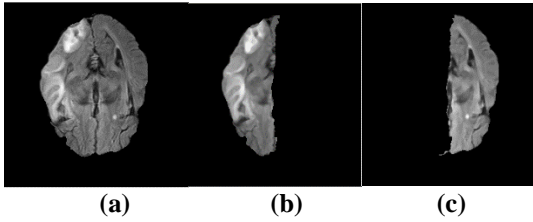


Fig. 2. Bifurcation phase: (a) Input MRI Slice (b) Left Portion (c) Right portion

With respect to the first sample presented in Fig. 3, an interesting pattern could be observed while moving from 11th bin to 14th bin. This increase in difference of pixels between the left and the right portion is observed from 11th to 12th bin. Then, the rate of difference decreases from 12th bin to 13th bin. Again it continues to increase from 13th to 14th bin. Similarly, for the second sample presented in Fig. 3, the rate of difference decreases from 11th to 12th bin. Then, it increases from 12th to 13th bin. Again it continues to decrease from 13th to 14th bin. Hence, an extensive analysis is done on the information present in 13th bin to analyse this change in the direction of pattern. The information present in 13th bin is alone reconstructed according to the relation presented in Eq. 3.

$$C_{k=13}(x, y) = I(x, y) .* BP_{k=13}(x, y) \quad (3)$$

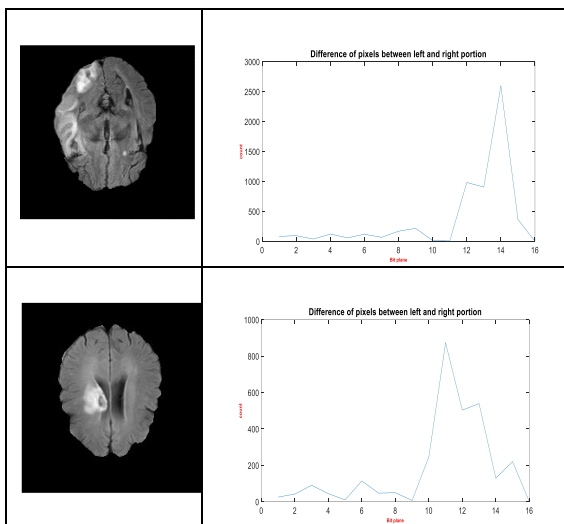


Fig. 3. Analysis on difference of pixels between left and right portion.

In order to examine the information present in the reconstructed image of 13th plane, histogram of the reconstructed image is calculated as presented in Eq. 4.

$$C(r_k) = n_k \quad (4)$$

where L = number of gray levels in the image

$$k = 0, 1, 2, \dots, L-1$$

n_k = count of pixels with gray level 'r_k'

Fig. 4 presents the histogram distribution of pixels (plot of $C(r_k)$ vs n_k grouped under 256 bins) in the reconstructed image of 13th bit plane for the image presented in Fig 2.

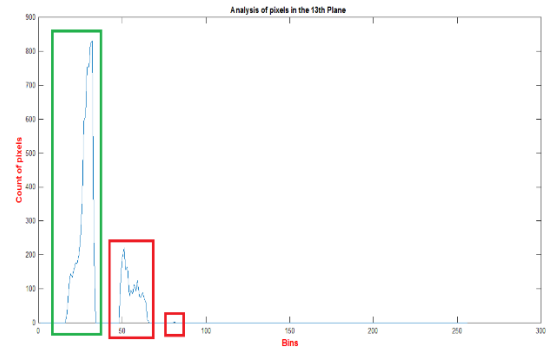


Fig. 4. Histogram distribution of pixels in the 13th bin.

It could be observed that in the 13th plane, there is more than one mode of gray level distribution of intensities. The information corresponding to each mode is clearly presented in Fig 5. Based on the analysis carried with different datasets, it was inferred that the first mode refers to the content of the normal brain tissues. Starting from the second mode, the details of the lesion could be captured and these details are redundant in the next plane also (i.e. 14th plane).

In the 15th plane, the details of the infarct lesion are clearly visible. But it could be noted that, the boundaries and the surrounding regions of the lesion are partially captured in the 15th plane and these details are available in the higher modes of the histogram of the 13th plane. This is due to the fact that, the tissues surrounding the central core will have progressive change in their intensity in due course. Hence these subtle details surrounding the core should also be extracted to fully represent the segmented region. Hence an adaptive filter function ' $F(x, y)$ ' is defined based on the information obtained through the above analysis and it is presented in Eq. 5.

$$F(x, y) = \begin{cases} 0 & \text{if (pixels in mode = 1 of histogram}(C_{k=13}(x, y))) \\ 1 & \text{if (pixels in modes > 1 of histogram}(C_{k=13}(x, y))) \\ 1 & \text{for } C_{k=15}(x, y) \end{cases} \quad (5)$$

Where,

$$C_{k=15}(x, y) = I(x, y) .* BP_{k=15}(x, y)$$

Finally, the segmented region of interest ' $R(x, y)$ ' is obtained with the help of relation presented in Eq. 6.

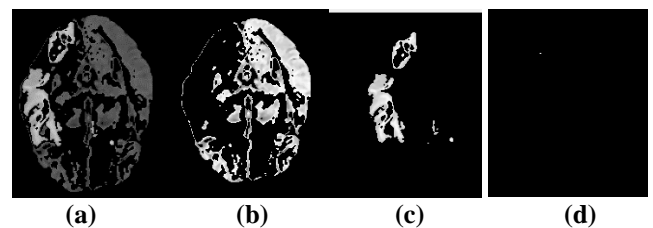


Fig. 5. (a) Reconstructed image with 13th bin (b) Content corresponding to first mode (c) Content corresponding to second mode (d) Content corresponding to third mode.

$$R(x, y) = I(x, y) .* F(x, y) \quad (6)$$

The details of these bit planes are clearly presented in Fig. 6. Hence in order to segment the lesion portion, the information present in higher modes of the 13th plane are combined with the information present in the 15th plane and the resultant segmented region of interest is highlighted in Fig. 7.



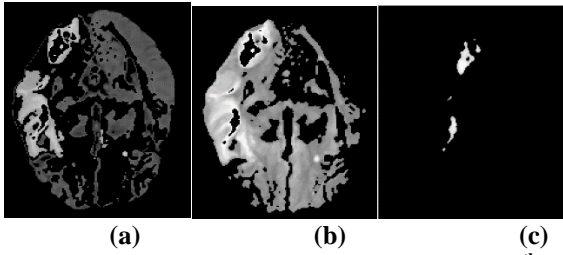


Fig. 6. (a) Reconstructed image with 13th bin
(b) Reconstructed image with 14th bin
(c) Reconstructed image with 15th bin

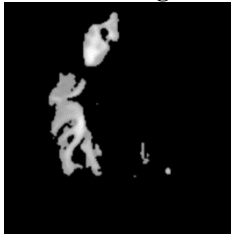


Fig. 7. Final segmented lesion using SBPPS.

Feature Extraction

in the Curvelet domain. As Curvelet transform is well suited to describe curve singularities, extracting co-occurrence matrix based features in Curvelet space can act as an efficient texture descriptor for describing the texture of the brain tissues. Curvelet transform is basically a multi-scale transform which could represent curve singularity details in an efficient way. The continuous Curvelet transform is defined based on a radial window: $W(r)$ and an angular window: $V(t)$. ‘ W ’ represents a frequency-domain variable, and ‘ r ’ and ‘ θ ’ are used to represent the polar coordinate space. These two windows are real valued non-negative functions with ‘ W ’ taking positive real arguments and supported on $r \in (1/2, 2)$ and ‘ V ’ having real arguments and supported on $t \in [-1, 1]$.

A polar wedge ‘ U_j ’ is basically constructed with the help of two factors ‘ W ’ and ‘ V ’. It could be defined in the Fourier space as per the Eq. 7.

$$U_j(r, \theta) = 2^{-\frac{3j}{4}} W(2^{-j}r) V\left(\frac{2^{\frac{j}{2}}\theta}{2\pi}\right) \tag{7}$$

The continuous Curvelet transform ‘ φ ’ is now defined using three parameters namely scale 2^{-j} , position $x_k^{(j,l)}$, and orientation θ_l . Mathematically, it is defined as per the relation presented in Eq. 8.

$$\varphi_{j,l,k}(x) = \varphi_j \left(R_{\theta_l} \left(x - x_k^{(j,l)} \right) \right) \tag{8}$$

Discretization of this continuous version of Curvelet transform was carried out by Candes and Donoho with the help of a wrapping approach. A rectangular grid is used to convert the continuous Curvelet in each scale and angle to Cartesian form. The discrete Curvelet coefficients are defined as presented in the Eq. 9.

$$C(j, l, k) = \sum f [t_1, t_2] \overline{\varphi_{j,l,k}^d [t_1, t_2]} \tag{9}$$

further by examining the second order features namely co-occurrence matrix based features in Curvelet space and these features were named as Curvelet Co-occurrence Matrix features. 13 features were extracted to describe the texture properties in Curvelet space. It includes Autocorrelation, Contrast, Correlation, Cluster Prominence, Cluster shade, Dissimilarity, Energy, Entropy, Homogeneity, Maximum

Probability, Information measure of correlation, Inverse difference normalized and Inverse difference moment normalized. Curvelet transform is applied to the segmented output and the resultant tiling structure in five different scales is presented in Fig. 8.

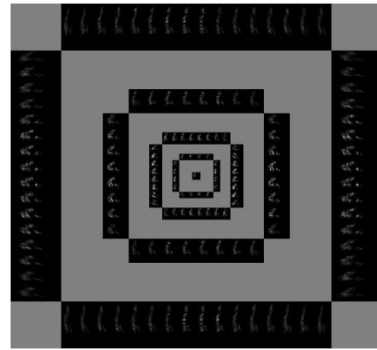


Fig. 8. Discrete Curvelet tiling obtained for the segmented output present in Fig. 7.

Classification

This research employs SVM for classifying the input feature vector. The proposed work extracts co-occurrence matrix based features. Let the input feature vector be denoted as X_i which is of the length $[1, 2, \dots, M]$. Let the two class labels be denoted as ω_1 and ω_2 . This classification algorithm basically examine the given input vectors and construct an optimal hyper plane ‘ $g(x)$ ’ to differentiate the two classes ω_1 and ω_2 . The relation for the constructed hyperplane is presented in Eq. 10.

$$g(x) = W^T x + W_0 = 0 \tag{10}$$

Linear, Radial Basis Function (RBF), sigmoid and polynomial kernel functions were utilized to train the classifier in this work. CCM features extracted in the Curvelet space are given as input to SVM and a classification model is developed. If the classification model identifies a given sample as abnormal, post process segmentation using SBPPS is applied to that particular slice to delineate the lesion.

III. RESULTS AND DISCUSSION

The proposed work consists of two major steps namely: SBPPS for segmentation and CCM features for detection. The performance of these two algorithms is examined with the help of suitable performance metrics.

Segmentation

The performance of the segmentation process is verified with the help of measures like Dice Coefficient (DC) and Structural Similarity Index (SSIM). The Dice’s coefficient is used to measure the degree of similarity between two different samples. It basically returns a value between 0 and 1. A value of ‘0’ denotes that there is no similarity between the samples whereas a value of ‘1’ reflects a perfect similarity between them. The dice’s coefficient is given by the relation presented in Eq. 11.

$$DC = \frac{2|A \cap B|}{|A| + |B|} \tag{11}$$

where ‘ A ’ and ‘ B ’ represents the two given samples to be compared.



The Structural Similarity index is another objective measure used to compare image similarity. It is determined according to the relation present in Eq. 12.

$$SSIM(x, y) = \frac{(2\mu_x\mu_y + C_1)(2\sigma_{xy} + C_2)}{(\mu_x^2 + \mu_y^2 + C_1)(\sigma_x^2 + \sigma_y^2 + C_2)} \quad (12)$$

Where μ_x & μ_y represents the average of x and y. σ_x & σ_y represents the variance of x and y. The parameters C1 and C2 are used to stabilize the division operation.

The segmented output is compared with ground truth reference using these two metrics and the observations are highlighted for few best samples in Table 1.

While the proposed SBPPS approach is able to detect scattered lesions and hyper-intense structures of varying degree, it also extracted few non-lesion areas like gliosis. Fig. 9 presents the observation for one such sample, where the gliosis is extracted along with lesion area. This can be considered as a limitation of the proposed SBPPS approach.

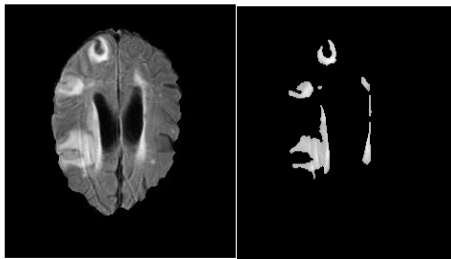


Fig. 9. Detection of hyper intense structures along with gliosis.

Classification

Both RBF and Sigmoid kernel exhibited better performance when compared to other two kernel functions. These results are highlighted in Fig. 10. The accuracy of the proposed work is compared against various existing approaches and the results are highlighted in Table 2. It could be observed that the proposed method is highly accurate when compared to other methods.

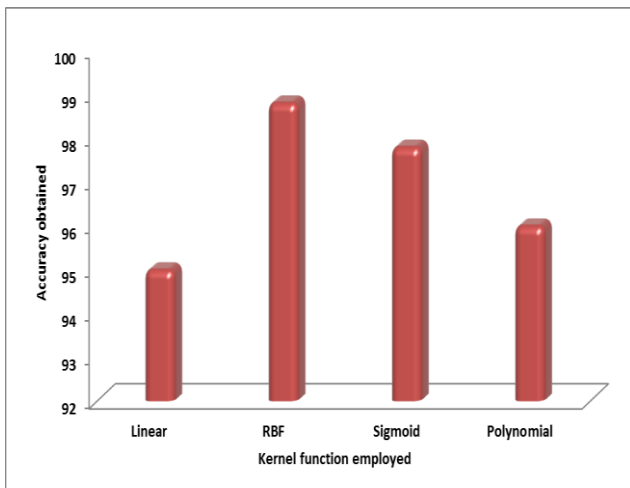


Fig. 10. Comparison of classification accuracy with different kernel functions.

Table 1. Performance Comparison of segmentation phase.

Input Image	Segmented Output	Ground Truth	DC	SSIM
			0.9718	0.9788
			0.9798	0.9801
			0.9812	0.9672
			0.9862	0.9901
			0.9874	0.9921

Table 2. Comparison of classification accuracy

S. No	Source	Features	Classifier	Accuracy reported
1	Fuk-hay et al. [8]	GLCM based measures	ANN	94.4
2	AsitSubudhi et al. [14]	Statistical and Geometrical features	Random forest classifier	85
3	Gupta et al. [25]	GLCM based measures	Artificial Neural Networks	98
4	Hema Rajini et al. [13]	GLCM based measures	SVM	98
5	Sivakumar et al. [23]	Texture and morphological features	ANFIS	98.7
6	Proposed approach	Curvelet co-occurrence matrix features	SVM	98.81

IV. CONCLUSION

A novel approach for detection and delineation of ischemic lesion from brain MRI images is proposed in this work. An extensive analysis was carried on the bit plane pattern obtained from multiple datasets. By combining the symmetry property and pattern derived through the bit plane analysis, an adaptive filter function is designed using the proposed SBPPS algorithm to delineate the lesion structures even with varying intensity profile. The co-occurrence matrix based features extracted in Curvelet space was able to quantify and represent the hyper-intense nature of the ischemic lesions with an accuracy of 98%.



This research was focussed towards the delineation of ischemic lesion. It was able to extract even scattered lesions. Also, the time taken to delineate such complex structures is considerably reduced when compared to traditional methods which require proper initialization parameters from user.

REFERENCES

1. Leiva-Salinas C, Wintermark M. Imaging of Ischemic Stroke. *Neuroimaging clinics of North America*. 2010; 20(4):455-468.
2. Wardlaw JM, Murray V, Berge E, et al. Recombinant tissue plasminogen activator for acute ischaemic stroke: an updated systematic review and meta-analysis. *Lancet* 2012; 379:2364-2372.
3. Overgaard, Karsten. The Effects of Citicoline on Acute Ischemic Stroke: A Review. *Journal of Stroke and Cerebrovascular Diseases*. 2014; 23(7):1764 – 1769.
4. Caligiuri, M.E., Perrotta, P., Augimeri, A. et al. Automatic Detection of WhiteMatterHyperintensities in Healthy Aging and Pathology Using Magnetic Resonance Imaging:A Review. *Neuroinform*. 2015; 13: 261.
5. R. Karthik & R. Menaka: Computer-aided detection and characterization of stroke lesion – a short review on the current state-of-the art methods. *The Imaging Science Journal*, 2018; 66(1):1-22.
6. Artzi, Moran et al. FLAIR lesion segmentation: Application in patients with brain tumors and acute ischemic stroke. *European Journal of Radiology*. 2013; 82(9):1512-1518.
7. Ghosh, N., Recker, R., Shah, A., Bhanu, B., Ashwal, S. and Obenaus, A.: Automated ischemic lesion detection in a neonatal model of hypoxic ischemic injury. *J. Magn. Reson. Imaging*, 2011; 33:772–781.
8. Fuk-hay Tang, Douglas K.S. Ng, Daniel H.K. Chow, An image feature approach for computer-aided detection of ischemic stroke, *Comput. Biol. Med*. 2011;41:529–536.
9. Nabizadeh N, John N, Wright C. Histogram-based gravitational optimization algorithm on single MR modality for automatic brain lesion detection and segmentation. *Expert Syst Appl*. 2014; 41:7820–7836.
10. Storelli L., Pagani E., Rocca M.A., Horsfield M.A., Filippi M.: A Semi-automatic Method for Segmentation of Multiple Sclerosis Lesions on Dual-Echo Magnetic Resonance Images. In: Crimi A., Menze B., Maier O., Reyes M., Handels H. (eds) *Brainlesion: Glioma, Multiple Sclerosis, Stroke and Traumatic Brain Injuries*. *BrainLes 2015*. Lecture Notes in Computer Science, 2016; 9556.
11. De Haan B, Clas P, Juenger H, et al. Fast semi-automated lesion demarcation in stroke. *NeuroImage*. 2014; 9:69–74.
12. Ghosh N, Sun Y, Bhanu B, et al. Automated detection of brain abnormalities in neonatal hypoxia ischemic injury from MR images. *Med Image Anal*. 2014; 18:1059–1069.
13. Hema Rajini N, Bhavani R. Computer aided detection of ischemic stroke using segmentation and texture features. *Measurement*. 2013; 46:1865–1874.
14. AsitSubudhi, Subhranshu Jena, SukantaSabut. Delineation of the ischemic stroke lesion based on watershed and relative fuzzy connectedness in brain MRI. *Med BiolEngComput*, 2017: 1-13.
15. R. Menaka, and R. Karthik.: A novel feature extraction scheme for visualisation of 3D anatomical structures. *Int. J. Biomedical Engineering and Technology*. 2016; 21(1):49-66.
16. S. Javeed Hussain, A. Satya Savithri and P. V. Sree Devi.: Segmentation of brain MRI with statistical and 2D wavelet features by using neural networks, 3rd International Conference on Trendz in Information Sciences & Computing (TISC2011), 154-159, 2011.
17. R.Karthik and R. Menaka.: A critical appraisal on wavelet based features from brain MR images for efficient characterization of ischemic stroke injuries. *Electronic Letters on Computer Vision and Image Analysis*, 2016; 15(3):1-16.
18. K. Hackmack, F. Paul, M. Weygandt, C. Allefeld, J.D. Haynes, Multi-scale classification of disease using structural MRI and wavelet transform, *Neuroimage*. 2012;62:48–58.
19. Karthik, R. and Menaka, R. “Statistical characterization of ischemic stroke lesions from MRI using discrete wavelet transformation”, *Transactions on Electrical Engineering, Electronics, and Communications*, Vol. 14, No. 2, pp. 57-64, 2016.
20. Karthik, R. Menaka, R. A Novel Brain MRI Analysis System for Detection of Stroke Lesions using Discrete Wavelets. *Journal of Telecommunication, Electronic and Computer Engineering*. Vol. 8 No. 5, pp. 49-53, 2016.
21. E. Candes, L. Demanet, D. Donoho, L. Ying, Fast discrete Curvelet transforms, *SIAM J. Multiscale Model. Simul*. 2006; 5(3):861–899.
22. Menaka. R, Chellamuthu. C and R. Karthik.: Efficient Feature point detection of CT images using Discrete Curvelet Transform, *Journal of Scientific and Industrial Research*. 2013; 72:312-315.
23. Sivakumar P, Ganeshkumar P. An efficient automated methodology for detecting and segmenting the ischemic stroke in brain MRI images. *Int. J. Imaging Syst. Technol*. 2017; 27:265–272.
24. Bhanu Prakash KN, Gupta V, Bilello M, et al. Identification, segmentation, and image property study of acute infarcts in diffusion-weighted images by using a probabilistic neural network and adaptive Gaussian mixture model. *AcadRadiol*. 2006; 13:1474–1484.
25. Gupta S, Mishra A, Menaka R. Ischemic stroke detection using image processing and ANN. *International Conference on Advanced Communication Control and Computing Technologies (ICACCCT)*; 1416–1420, 2014.
26. Bentley P, Ganesalingam J, Lalani A, et al. Prediction of stroke thrombolysis outcome using CT brain machine learning. *NeuroImage*. 2014; 4:635–640.
27. Karthik. R and Menaka. R.: A multi-scale approach for detection of ischemic stroke from brain MR images using discrete Curvelet transformation. *Measurement*. 2017; 100: 223-232.
28. Maier, O., Menze, B.H., von der Gabelntz, J., Häni, L., Heinrich, M.P., Liebrand, M., et al. ISLES 2015 - A public evaluation benchmark for ischemic stroke lesion segmentation from multispectral MRI Medical Image Analysis, 2017; 35:250-269.
29. Sheena XinLiu, Symmetry and asymmetry analysis and its implications to computer-aided diagnosis: A review of the literature. *Journal of Biomedical Informatics*. 2009; 42(6):1056-64.